Filling-factor-dependent cyclotron mass in space-charge layers on GaAs

E. Batke,* H. L. Störmer, A. C. Gossard, and J. H. English
AT&T Bell Laboratories, Murray Hill, New Jersey 07974-2070
(Received 17 March 1987)

We report frequency-domain studies of cyclotron resonance in electron space-charge layers on GaAs. We observe variations of the cyclotron mass correlated with the filling factor. This is discussed in terms of conduction-band nonparabolicity, spin splitting of the Landau levels, and filling-factor-dependent screening of the electron–optical-phonon interaction. In samples with mobilities lower than 5×10^5 cm^2/V s there are line-shape anomalies with characteristics of anti-level-crossing that do not scale with the filling factor but depend on the electron density itself.

Cyclotron resonance (CR) in single interface GaAs-$Al_xGa_{1-x}As$ heterostructures was studied by many authors.[1–6] Experiments in high magnetic fields demonstrated the importance of conduction-band nonparabolicity and a resonant polaron effect on the cyclotron excitation.[3,4] Different cyclotron resonance anomalies were observed and have led to a variety of interpretations. The importance of filling-factor-dependent screening[1] was pointed out, coupling to magnetoplasmons was suggested,[2,6] and it was speculated on an influence of the quantum Hall effect at fractional filling factors.[5] At present none of these interpretations is well established and there is no unified picture which could account for all anomalies observed in the CR position and linewidth. Here we investigate CR in electron space-charge layers on GaAs for samples of practically the same charge densities but with different mobilities. Our experiments demonstrate that the cyclotron mass correlates with the filling factor $f=2\pi l^2N_s$ (l represents the Landau orbit) and reveal a nontrivial dependence on the sample mobility.

In Table I the parameters of two representative samples are listed. The charge densities N_s and mobilities μ are determined by Shubnikov–de Haas and van der Pauw measurements, respectively. CR is investigated on wedged samples (5×5 mm^2) in far-infrared transmission of unpolarized radiation at a fixed magnetic field with a rapid scan Fourier-transform spectrometer. The experimental setup is described elsewhere.[7] Magnetic fields B in steps of about 0.1 T are chosen covering a range 1 T$\leq B\leq$12 T. The accuracy of the magnetic field strength was measured with nuclear magnetic resonance and is known to be better than 0.1%. The temperature is 4.3 K and the spectrometer resolution is set to 0.1 cm^{-1}. Special care is taken to orient the sample normal parallel to the magnetic field to reduce influences of CR–intersubband-resonance (ISR) coupling.[8] Information about the high-frequency magnetoconductivity is obtained from the relative change in transmission $\Delta T/T=[T(B_1)-T(B_2)]/\ T(B_2)$ by comparing two transmission spectra $T(B)$ measured at slightly different magnetic field strengths B_1 and B_2.

Figure 1(a) shows experimental $\Delta T/T$ for sample 1 in equal steps within the designated magnetic fields. Filling factors and ISR position are marked by arrows. In the spin polarized state $f<1$ the resonance profile is sharpest exhibiting a field-independent amplitude. Around $12T$ a broadening is observed, caused by coupling of the CR to ISR. Starting at $f=1$ the CR amplitude decreases with increasing filling factor and exhibits a minimum close to $f=2$. A second more pronounced minimum exists in the filling-factor regime $4>f>2$. In Fig. 1(b) for $4>f>2$ the CR line shape is shown on an expanded energy scale. Generally the line shapes are asymmetric and at $B=2.75$ T we observe the onset of a splitting. This particular line-shape anomaly depends on the sample mobility. It does not exist in high mobility samples beyond a mobility of roughly 5×10^5 cm^2/V s. In samples with mobilities lower than the one of sample 1 no splitting but a broadening is found. A qualitatively similar CR anomaly was observed in Ref. 2 and correlated with the charge density N_s. Our experiment confirms their N_s dependence and supports their finding that the phenomenon does not scale with filling factor. In addi-

TABLE I. Parameters of GaAs-$Ga_{1-x}Al_xAs$ heterojunctions 1 and 2. d_c, d_{A1}, and d_s represent the cap layer, doped $Al_xGa_{1-x}As$ layer ($n_{si}\approx1\times10^{18}$ cm^{-3}, $x\approx0.3$) and spacer thickness, respectively. E_{01} is the intersubband resonance energy and F_s the associated surface electric field in the triangular well potential approximation.

Sample	N_s (10^{11} cm^{-2})	μ (10^3 cm^2/V s)	d_c (Å)	d_{A1} (Å)	d_s (Å)	E_{01} (cm^{-1})	F_s (10^4 V/cm)
1	1.80±0.07	440	200	700	350	162	1.80
2	1.95±0.05	880	200	650	350	142	1.65

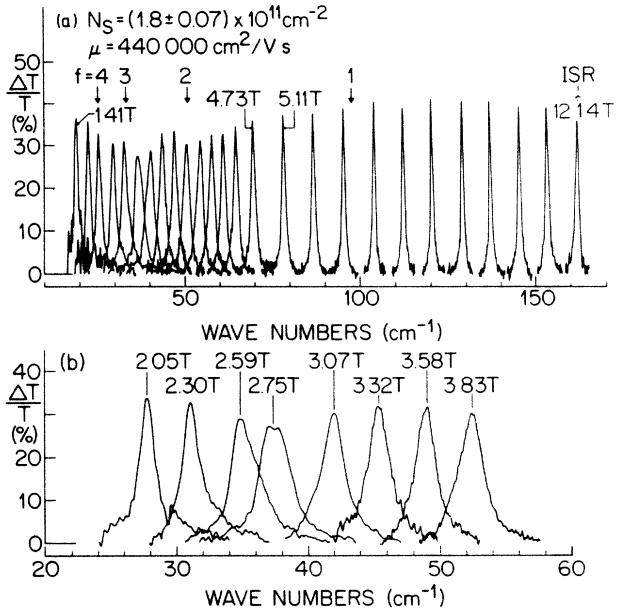

FIG. 1. Experimental cyclotron resonances for sample 1 at fixed magnetic fields B. (a) Magnetic field regime 1.41 to 12.14 T. Magnetic fields are stepped equally within the marked limits. Filling factors f and intersubband resonance position are marked by arrows. (b) Filling-factor regime $4>f>2$ of (a) shown on an expanded frequency scale.

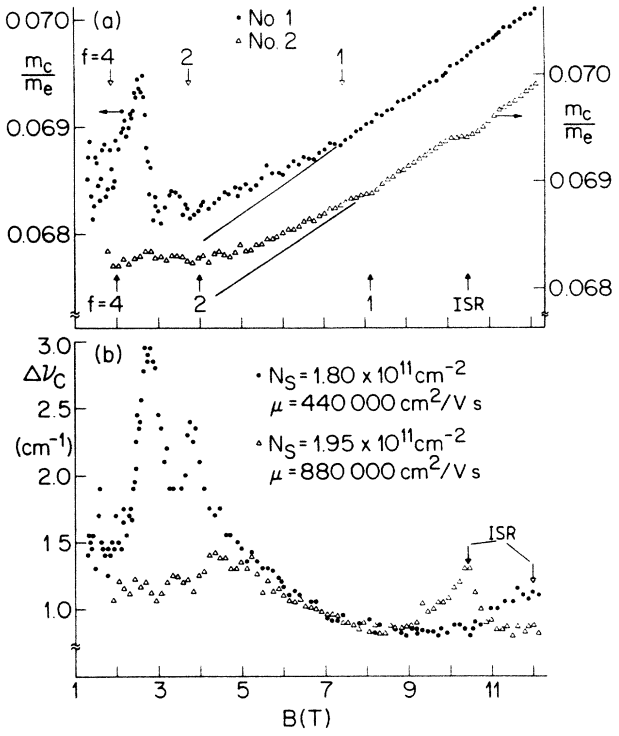

FIG. 2. (a) Cyclotron resonance masses m_c for samples 1 and 2. Filling factors and ISR position are marked by downward- and upward-pointing arrows for samples 1 and 2, respectively. Straight lines are guides to the eye indicating a change in mass slope at $f=1$. (b) Full width at half maximum $\Delta\nu_c$ for samples 1 and 2. Solid and open arrows mark ISR positions for samples 1 and 2, respectively.

tion, we find that this anomaly depends on the tilt angle of the sample and on the temperature. With increasing tilt angle and decreasing temperature the resonance splitting increases and shows characteristics of anti-level crossing. At present the participating excitation is unknown. Coupling to magnetoplasmons[2] seems unlikely, since for both the CR and the magnetoplasmon mode only the perpendicular magnetic field component is relevant[9] and a dependence of the coupling strength on the tilt angle is not expected.

In the following we concentrate on CR anomalies which correlate with the filling factor. In Fig. 2 we show CR positions characterized in terms of a cyclotron mass $m_c = eB/\omega_c$ and full widths at half maxima (FWHM) for both samples. Filling factors for samples 1 and 2 are marked in Fig. 2(a) by downward and upward-pointing arrows, respectively. Both samples are nearly equivalent for transitions from the lowest Landau level and show a mass increase starting at $f=2$ with increasing magnetic field strength. At $f=1$ the cyclotron mass slope changes and m_c increases linearly with B for the spin polarized state. In Fig. 2(a) the mass slopes in the spin polarized state are indicated by straight lines as guides to the eye. Both lines extrapolate to a mass value of $0.0671 m_e$ at $B=0$ T. Cyclotron mass variations due to CR-ISR coupling could be minimized for both samples by proper orientation and are only marginally visible for sample 2 around 10.5 T. In the high filling-factor regime $f>2$ the m_c variation with B is different for both samples. Sample 2 exhibits a constant m_c whereas for sample 1 there is a m_c enhancement close to $f=2$. The second more prominent mass enhancement for sample 1 in the regime $4>f>2$ is associated with a strong increase in FWHM and relates to the mobility-dependent anomaly discussed above [Fig. 1(b)].

CR line-shape broadenings underline the importance of filling-factor-dependent screening for our experiment. Whenever the Landau and/or spin-level broadening is smaller than the level separations, the efficiency of screening depends on the position of the Fermi energy with respect to the Landau ladder.[10-12] Screening is reduced whenever the Fermi energy is located in the tails of a Landau level, i.e., at filling factors $f=1,2,3,\ldots$, reflecting the density of states. Since the spin splitting is small compared to kT we are unable to detect anomalies at odd integers. CR broadenings, correlated with even integer filling factors, were recently observed on InAs for the high filling-factor regime $f \geq 6$.[13] A broadening of the CR is observed in our samples close to $f=2$ [Fig. 2(b)]. Within our accuracy we cannot confirm a line-shape broadening for $f=4$. Since screening depends sensitively on the density of states, a broadening at $f=4$ cannot be expected if there is considerable overlap of adjacent Landau levels, which is possible particularly in the low field limit. In addition, for our high mobility samples we have to remember that the FWHM is a complex function of the cyclotron

scattering time τ_c and the charge density N_s due to signal saturation.[7] For example, for sample 2 a 10% increase in FWHM would entail a 30% decrease in τ_c. Thus small changes in τ_c due to filling-factor-dependent screening may be masked by saturation. Assuming a classical Drude-type magnetoconductivity $\sigma^{\pm}=N_s e^2\tau_c/\{m_c[1+i(\omega\pm\omega_c)\tau_c\}$ and replacing τ_c by τ_{dc}, obtained from the mobility, the calculated FWHM for samples 1 and 2 are 1.25 cm^{-1} and 1.0 cm^{-1}, respectively. These calculated FWHM are in good agreement with the experimental values at low fields [Fig. 2(b)]. In the high field limit, particularly for the spin-polarized state $f\leq 1$, the CR is sharpened beyond the low field values. The sharpening of the CR for $f<2$ is in agreement with predictions based on screening and relates to the spacer thickness d_s and the bulk impurity concentration.[12] Generally, screening by the electrons does not affect the short-range part of the scattering potential. With a setback distance d_s scattering of the remote impurities is suppressed for wave vectors $q\geq 1/d_s$ and the remaining long-range part can be screened efficiently by the electrons. This process is strongest for the lowest Landau level and limited by the short-range scattering of the background impurities. For $f\leq 1$, if we neglect the broadening due to CR-ISR coupling, both samples are undistinguishable. Their FWHM and CR amplitudes are $\Delta\nu_c=0.8\pm0.05$ cm^{-1} and $\Delta T/T(\nu_c)=42\pm1.5\%$, respectively. Interestingly, the experimental $\Delta\nu_c$ for $f\leq 1$ is in excellent agreement with the FWHM of the Drude model in the limit $\tau_c\rightarrow\infty$. However, the experimental amplitudes are smaller than the saturation value of 50%. This observation might indicate residual inhomogeneity in our samples. Resonance halfwidths and amplitudes stay constant in the spin-polarized state which we verified up to $f\approx 0.3$ for samples with $N_s<10^{11}$ cm^{-2}. In our experiments there is no indication for CR anomalies related to fractional filling factors.

In the following we will show that the m_c increase for CR transitions from the lowest Landau level is a consequence of the nonparabolicity of the GaAs conduction band and that the population of the upper spin state contributes to the change in mass slope at $f=1$. To account for the conduction-band nonparabolicity of the GaAs system a $\mathbf{k}\cdot\mathbf{p}$ perturbation theory including coupling between multiple bands is required.[14] However, for simplicity we calculate the spin-split Landau energies $E_{n,\sigma}$ (n represents the Landau-level index and σ represents the spin) in the improved two-band model which includes the contributions of the remote bands via an effective energy gap E_g^*. For details of our calculation we refer the reader to Ref. 3. From the calculated $E_{n,\sigma}$ a cyclotron mass

$$m_{cn\sigma}=\frac{\hbar eB}{E_{n+1,\sigma}-E_{n,\sigma}}$$

is defined. Figure 3(a) shows results for $m_{cn\sigma}$ together with some CR transitions $n,\sigma\rightarrow n+1,\sigma$. The parameters used in the calculation are summarized in Fig. 3(b). The surface electric field F_s is chosen from sample 2 and is estimated from the measured ISR energy E_{01} in the triangular well potential approximation (see last column of Table I). The effective g factor is included in the form $g^*=-0.44+0.1(n+0.5)$ which approximates the expression of Ref. 15. The best description of the experiment is obtained with the bare band-edge mass $m_0=0.0655m_e$ and an effective energy gap $E_g^*=850$ meV. Since the spin splitting is not resolved in our experiment, we define an average cyclotron mass as

$$\langle m_c\rangle\equiv\sum_{n,\sigma\rightarrow n+1,\sigma} n_{n\sigma}m_{cn\sigma}\ ,$$

which is the sum of all $m_{cn\sigma}$ weighted with the relative occupation $n_{n\sigma}$ of the spin-split Landau levels n and σ. The calculated $\langle m_c\rangle$ [Fig. 3(b)] reproduces all features of the experimental values for sample 2 [Fig. 2(a)]. The dashed line in Fig. 3(b) indicates the cyclotron mass slope of the spin-polarized state. In the filling-factor regime $2>f>1$ the population of the upper spin state decreases the cyclotron mass slope of the spin polarized state. Our calculation is strictly valid only at zero temperature. In our experiment, however, there is a thermal smearing of 0.36 meV which is comparable to the size of the spin splitting (0.25 meV at 10 T assuming the bulk g factor at the band edge). In the presence of thermal smearing the higher spin state is also populated for $f<1$

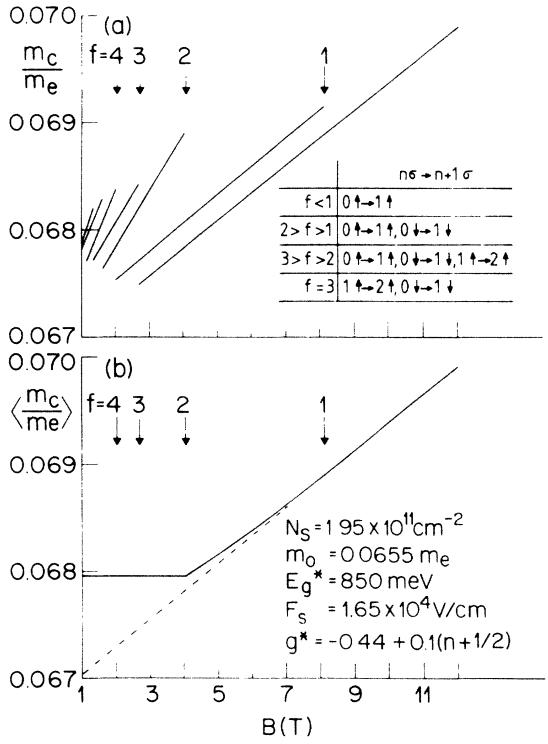

FIG. 3. Calculated cyclotron masses m_c vs magnetic field strength B. (a) Spin splitting is resolved. The inset lists some CR transitions. (b) Average $\langle m_c\rangle$ obtained by weighing the mass values of (a) with the relative occupation of the participating spin-split Landau levels. The dashed line is a guide to the eye indicating the change in mass slope at $f=1$. Filling factors f are indicated by arrows and the parameters for the calculation are listed in the inset.

and the change in mass slope at $f=1$ is reduced as compared to the calculation. The influence of thermal smearing can only be suppressed if the exchange enhancement[16] of the g factor, which can increase the spin-splitting considerably, is incorporated. However, the experimental change in mass slope is about a factor of 3 too large to be explained by nonparabolicity of the g factor alone. As a possible explanation for this discrepancy we propose coupling of the electrons to the longitudinal optical phonons in GaAs.

If screening of the electron-phonon interaction is neglected, polaron effects are stronger in two-dimensional (2D) than in three-dimensional (3D) systems. We tested the influence of polaron coupling on our experiment with the unscreened two-dimensional polaron mass correction [see Eq. (13) of Ref. 17]. Taking the bulk value of the Fröhlich coupling constant $\alpha=0.07$ we obtain cyclotron masses about 2.7% higher than those of Fig. 3(a). It requires an unacceptable reduction of m_0 to achieve agreement between experiment and theory for $\alpha=0.07$. Therefore, in our magnetic field regime polaron effects must be reduced compared to the 3D case, indicating the importance of screening. In a simplified picture, neglecting a possible influence of the Pauli principle on the polaron effect,[18] but assuming a filling-factor-dependent screening of the electron-phonon interaction, we expect cyclotron mass enhancements at even integer filling factors. For example, the cyclotron mass enhancement for sample 1 close to $f=2$ [Fig. 2(a)] could be explained under such circumstances. Since screening is most efficient in the spin-polarized state, little or no polaron effect is expected in this case. In the filling-factor regime $2>f>1$ screening would result in a reduced polaron effect with decreasing f. Thus filling-factor-dependent screening of the electron-phonon interaction can contribute to the different cyclotron mass slopes in the filling-factor regimes $2>f>1$ and $f\leq 1$.

In conclusion, CR experiments on single interface heterostructures on GaAs reveal a nontrivial sample dependence. In samples with mobilities below 5×10^5 cm^2/V s CR anomalies exist which depend on N_s and exhibit features of anti-level crossing. Generally, field-dependent line-shape variations confirm the importance of filling-factor-dependent screening. Cyclotron masses can be explained by a combination of band nonparabolicity, spin splitting, and possibly filling-factor-dependent screening of the electron-phonon interaction.

---

*Present address: Institut für Angewandte Physik, Universität Hamburg, Jungiusstrasse 11, D-2000 Hamburg 36, West Germany.

[1]T. Englert, J. C. Maan, C. Uihlein, D. C. Tsui, and A. C. Gossard, J. Vac. Sci. Technol. B **1**, 427 (1983); Solid State Commun. **46**, 545 (1983).

[2]Z. Schlesinger, S. J. Allen, J. C. M. Hwang, P. M. Platzmann, and N. Tzoar, Phys. Rev. B **30**, 435 (1984).

[3]M. Horst, U. Merkt, W. Zawadzki, J. C. Maan, and K. Ploog, Solid State Commun. **53**, 403 (1985).

[4]H. Sigg, P. Wyder, and J. A. A. J. Perenboom, Phys. Rev. B **31**, 5253 (1985).

[5]G. L. J. A. Rikken, H. W. Myron, P. Wyder, G. Weimann, W. Schlapp, R. E. Horstmann, and J. Wolter, J. Phys. C **18**, 1175 (1985).

[6]Z. Schlesinger, W. I. Wang, and A. H. MacDonald, Phys. Rev. Lett. **58**, 73 (1987).

[7]E. Batke, D. Heitmann, and C. W. Tu, Phys. Rev. B **34**, 6951 (1986).

[8]Z. Schlesinger, J. C. M. Hwang, and S. J. Allen, Phys. Rev. Lett. **50**, 2098 (1983).

[9]C. Kallin and B. I. Halperin, Phys. Rev. B **30**, 5655 (1984).

[10]S. Das Sarma, Phys. Rev. B **23**, 4592 (1981).

[11]R. Lassnig and E. Gornik, Solid State Commun. **47**, 959 (1983).

[12]T. Ando and Y. Murayama, J. Phys. Soc. Jpn. **54**, 1519 (1985).

[13]D. Heitmann, M. Ziesmann, and L. L. Chang, Phys. Rev. B **34**, 7463 (1986).

[14]F. Thiele, U. Merkt, J. P. Kotthaus, G. Lommer, F. Malcher, U. Rösseler, and G. Weimann, Solid State Commun. **62**, 841 (1987).

[15]G. Lommer, F. Malcher, and U. Rössler, Phys. Rev. B **32**, 6965 (1985).

[16]T. Ando, J. Phys. Soc. Jpn. **37**, 622 (1974).

[17]F. M. Peeters, Wu Xiaoguang, and J. T. Devreese, Phys. Rev. B **34**, 1160 (1986).

[18]D. M. Larsen, Phys. Rev. B **30**, 4595 (1984).